Objective Optimization of Weather Radar Networks for Low-Level Coverage Using a Genetic Algorithm

JAMES M. KURDZO AND ROBERT D. PALMER

School of Meteorology, and Atmospheric Radar Research Center, University of Oklahoma, Norman, Oklahoma

(Manuscript received 8 April 2011, in final form 22 November 2011)

ABSTRACT

The current Weather Surveillance Radar-1988 Doppler (WSR-88D) radar network is approaching 20 years of age, leading researchers to begin exploring new opportunities for a next-generation network in the United States. With a vast list of requirements for a new weather radar network, research has provided various approaches to the design and fabrication of such a network. Additionally, new weather radar networks in other countries, as well as networks on smaller scales, must balance a large number of variables in order to operate in the most effective way possible. To offer network designers an objective analysis tool for such decisions, a coverage optimization technique, utilizing a genetic algorithm with a focus on low-level coverage, is presented. Optimization is achieved using a variety of variables and methods, including the use of climatology, population density, and attenuation due to average precipitation conditions. A method to account for terrain blockage in mountainous regions is also presented. Various combinations of multifrequency radar networks are explored, and results are presented in the form of a coverage-based cost–benefit analysis, with considerations for total network lifetime cost.

1. Introduction

As the current Weather Surveillance Radar-1988 Doppler (WSR-88D) radar network approaches the end of its expected lifetime (Yussouf and Stensrud 2008), numerous studies have raised several opportunities for improvement in a future network. Of principle interest is decreasing the time needed to complete a full volume scan in order to provide forecasters with more time and data for issuing warnings. Multiple proposals for a new Multimission Phased Array Radar (MPAR) network have attempted to address this desire (Weber et al. 2007; Zrnić et al. 2007). Additionally, improvements in the low-level scanning height in a new radar network are possible if the operational range of individual radars is less than the current 460-km range of the WSR-88D systems and radar sites are located closer to each other. The Collaborative and Adaptive Sensing of the Atmosphere (CASA) program proposes the use of low-cost X-band polarimetric radars that could be placed less than 20 km apart in order to observe a greater portion of the boundary layer nationwide (McLaughlin et al. 2009). Additionally, the CASA concept aims to provide collaborative, adaptive capabilities in a weather radar network, resulting in faster scan updates for the most weather-impacted areas. Such a network could also be capable of providing low-level wind field observations for rapid-update mesoscale models, in order to provide warn-on-forecast support for the National Weather Service (Stensrud et al. 2009).

Whether long-range S-band radars or shorter-range X-band radars (or a combination thereof) are used in a future network, the total cost, including production, maintenance, and operation, will be an important factor. S-band radars, such as those currently being used in the WSR-88D network, are typically priced at a relatively substantial level, while X-band radars operating at a low power are expected to cost considerably less. However, being placed only 20 km apart, the cost of such an X-band network may also exceed viable funding amounts solely because of the number of radars that would be required. Therefore, it is prudent to fabricate a network that offers as many improvements to current networks as possible, while remaining fiscally sound.

One option, which could offer numerous improvements while potentially keeping costs low, would be to

Corresponding author address: James M. Kurdzo, Atmospheric Radar Research Center, University of Oklahoma, 120 David L. Boren Blvd., Suite 4600, Norman, OK 73072.
E-mail: kurdzo@ou.edu

DOI: 10.1175/JTECH-D-11-00076.1

utilize a multifrequency network design in order to offer long-range coverage for more expensive S-band systems, while supplying short-range, X-band coverage in areas not covered at low-levels by S-band systems. A need therefore exists to optimize such a multifrequency network, in order to maximize coverage while minimizing cost. Through a series of optimizations, a cost-benefit analysis can be completed, informing network designers as to the most cost-effective network possibilities (in the case of this paper, ''benefit'' refers to coverage). Other radar network designs may also gain from similar optimizations, including single-frequency networks aiming simply for maximum areal coverage, as well as smaller networks optimizing for a particular coverage field such as population.

Observation network design, and coverage optimizations in general, are not new problems. Cellular tower placement presents a very common coverage problem, which has been solved in a variety of ways (e.g., Raisanen and Whitaker 2003; Thornton et al. 2003; Amaldi et al. 2008). Because of the large, complex nature of cellular networks, simulation tools are not sufficient; optimization algorithms [specifically genetic algorithms (GAs)] are capable of handling these problems (Lieska et al. 1998). Lieska et al. (1998) argued that genetic algorithms process the computer's representation of potential solutions directly, leading to a more rapid convergence to a solution. A fixed number of base stations (possible siting locations) in a gridded format were used, further limiting the computational complexity.

Genetic algorithms have also been used by Du and Bigham (2003) for cellular network optimization, with a specific emphasis on balancing traffic load using geographic variables. The study focused on optimizing coverage sizes and shapes in order to efficiently handle common traffic demand patterns. It was found that with the correct input parameters, genetic algorithms provided a relatively rapid convergence to an acceptable solution. Jourdan and de Weck (2004) also concluded, through significant review of various optimization methods, that genetic algorithms were the most suitable fit for a coverage study in which grid points are predetermined for coverage testing. In their case, the goal was to develop coverage patterns for aircraft-dropped, ad hoc wireless sensor networks.

In terms of weather radar network planning, there is limited literature regarding coverage optimization and radar siting using numerical methods. Leone et al. (1989) selected WSR-88D sites based upon various criteria, including severe weather climatology and distance from population centers. However, numerical optimization was not used, and a relatively small number of potential siting areas were considered. Ray and Sangren (1983) proposed planning small, multiple-Doppler networks for research purposes using a search algorithm. This was feasible for relatively small radar networks (less than 10 radars), but with the number of variables being utilized, a more expansive network could become problematic, simply because of the computation time needed for exhaustive search techniques.

Minciardi et al. (2003) presented the use of a genetic algorithm for planning an Italian weather radar network. Again, a relatively small number of potential sites were identified as viable options to locate radar systems. The advantages and disadvantages of each site were weighted and used in an optimization problem that determined the optimal placement of sensors based on the input parameters; this was termed ''site eligibility.'' The study was principally designed as a decision support system, with focus on one radar frequency and a limited set of potential siting locations.

In this paper, a genetic optimization algorithm capable of maximizing coverage within set physical boundary conditions is presented, using any combination of frequencies/ranges, and using any two-dimensional, quantifiable field as an optimizable quantity, such as those in Leone et al. (1989). The algorithm is applied to numerous real-world examples, including optimization based on combined population density and tornado probability, open-space coverage, and coverage with a simple terrain model. Testing is focused on low-level coverage examples, yielding shorter-range assumptions for low-frequency radars. The first result is provided as a basic example, while the remaining two results are analyzed in the form of a cost–benefit analysis, with stress placed on the decision support nature of the results, as in Minciardi et al. (2003) and Raisanen and Whitaker (2003). Conclusions are drawn regarding advantages and disadvantages of using multiple frequencies in each of the last two situations.

2. Optimization framework using a genetic algorithm

An optimal radar network must offer the most coverage possible, while minimizing cost, which is directly related to the number of radars. The coverage model, or fitness function, must be accurately quantifiable, capable of being evaluated over a large domain, and computationally inexpensive. Computational complexity results in slow processing speeds, meaning in order to keep speeds reasonable, it is impossible to offer every possible location within the domain as a siting location. Because of these necessities and limitations, a gridded format of sites

was deemed to most suitably fit our needs. Over the domain of the optimization, a gridded system with 0.1° of latitudinal and longitudinal spacing is defined. Each grid point represents both a potential radar site location *and* a location for testing coverage. Since this results in a finite domain, it is plausible to expect to achieve close to a global maximum in fitness without the need for excessive computing power.

Every optimization problem has different characteristics, leading to the need to explore all of the optimization techniques available in order to fit the needs of the problem. There are a number of global optimization techniques available; however, it was the goal of this work to identify one technique and develop a robust algorithm tailored to our needs. To identify the general technique for our problem, numerous optimization methods were explored. Multistart methods (Boender et al. 1982) utilize local optima search techniques, with searches beginning at many points along the solution curve. This leads to many ongoing searches at once, and a tax on computational complexity for large domain problems such as ours. Various linear programming methods exist (Dantzig and Thapa 1997; Karmarkar 1984), including the simplex algorithm (efficient method of finding a ''feasible region,'' but nondesirable results for large domains) and interior point optimization (similar to the simplex algorithm, but searches a greater depth of the feasible region). Nonlinear programming methods, such as the quasi-Newton approach (via use of gradient vectors), Nelder–Mead method (similar to the simplex algorithm), and the trust-region technique (which only searches a portion of the objective function) provide systems that allow for nonlinear constraints, similar to those in our problem (Shanno 1970; Nelder and Mead 1965; Celis et al. 1984).

Evolutionary algorithms represent a general concept that encompasses numerous types of optimization techniques (Eiben and Smith 2007). Genetic algorithms, specifically, are designed to be capable of finding global optimum solutions to complicated, nonlinear, real-world problems. Additionally, genetic algorithms have the ability to remain computationally inexpensive for simple problems, or to be developed into sophisticated algorithms capable of solving advanced problems. Genetic algorithms offer one of the most consistent methods to achieve global optimum, while also being flexible enough to accommodate real-world boundary conditions (Holland 1975).

The need for a global optimum, along with promising results from Du and Bigham (2003), Jourdan and de Weck (2004), and Lieska et al. (1998), resulted in the choice of a genetic algorithm for optimization. Genetic algorithms utilize the theory of evolution in order to progressively improve the functionally defined fitness. While it is certainly possible that other methods could result in more accurate–timely computations, genetic algorithms provided a reputable technique to build a test-case algorithm for the problem at hand. In our case, the population is defined as an array containing the latitudinal and longitudinal coordinate for each radar (each coordinate is a population member). Individual population members are stored as a floating-point representation (as opposed to binary), and are altered using random number generation (as opposed to bit replacement; Eiben and Smith 2007).

Between each generation, a portion of the population with the lowest fitness is discarded, and the remaining population members are randomly paired to create ''children'' (this is termed ''crossover''). A key feature of genetic algorithms is the ability to avoid local maxima in fitness. To achieve this, occasional mutations are introduced with a predetermined likelihood of occurrence. Additionally, in order to guarantee the lack of regression in fitness, the top two population members with the highest fitness, or ''elite members,'' are retained through each generation. Generations continue until a maximum fitness score is obtained; this maximum is recognized by a lack of change in the best fitness score for a predetermined number of generations, indicating convergence to a solution, and the end of the optimization.

A unique strength of the GA framework is the ability to apply the technique to a wide variety of real-world problems. In addition, in the case of a network coverage problem, there are various ways to represent population members and a fitness function. For the application presented here, a gridded system is utilized, which has numerous advantages. First, the search field can be limited to a domain as large or as small as computationally feasible. Second, boundary conditions can be easily imposed. Last, a gridded domain allows for unique applications of coverage and fitness function representations, making it simple to add value to the coverage problem. Each of these advantages will be explored in depth in the following discussion.

The application of a grid for the case at hand involves using a simple binary system to assess coverage. The gridded resolution used is 0.1° of latitude and longitude. Each point along the grid represents both a possible siting location and a location to assess coverage. This means that any radar can be located (its center coordinates) at a latitudinal and longitudinal position that is a multiple of the 0.1° resolution. When a radar is placed at a site, a theoretical circle is drawn that represents the expected range of the given radar.

This range may be based on power return degradation or the desired maximum height of the radar beam above ground level. For example, the range of a WSR-88D S-band radar is approximately 460 km; however, if low-level coverage is desired, the vertical cutoff height may be 1 km, effectively limiting the range of the radar to approximately 75 km.

After the circle for coverage is drawn for a radar site, the algorithm tests all grid points in order to determine if they are encompassed in the circle. If a point is in the circle, it is assigned a value of one. If it is not within the circle, it is assigned a value of zero. This simple, binary encoding technique allows for rapid computation of coverage for not only one radar, but all of the radars that may be placed inside the domain. The fitness function used sums the values of all of the grid points, resulting in a higher fitness score when more points are covered. This means that if multiple radars are overlapping, successive generations will work to ''spread'' the radars in order to provide more covered points. In this fashion, accounting for overlapping coverage as a penalty is not necessary, further reducing the computational complexity of the algorithm. A graphical representation of the fitness function and gridded system is shown in Fig. 1.

By limiting the number of grid points used for placing radars and testing for coverage to 0.1° resolution, the total search space can be limited significantly, leading to reduced computational complexity. While this system uses binary variables for each grid point, it is also possible to enhance the fitness score based upon weighted ''fields.'' These enhancements allow a designer to optimize a network based on very specific needs, and the gridded system is an integral part of the capability to perform such optimizations. The population members are represented via a concatenated array that contains the latitudinal and longitudinal coordinates for each radar in the optimization. Each member represents one set of radar locations, resulting in one fitness score for each network. As the members are combined and mutated through generations, new sets of radar locations are created in order to test for more optimal solutions. Figure 2 offers a concise description of the steps the algorithm takes in order to reach an optimal solution.

For each case presented, a population size of 750 and an elite count of two are used. Of the remaining 748 population members in the generation, approximately 80% are created via crossover, and approximately 20% are created via mutation. The genetic algorithm places a set number of radars at each frequency inside the gridded domain, while the fitness function determines which points are covered at each generation.

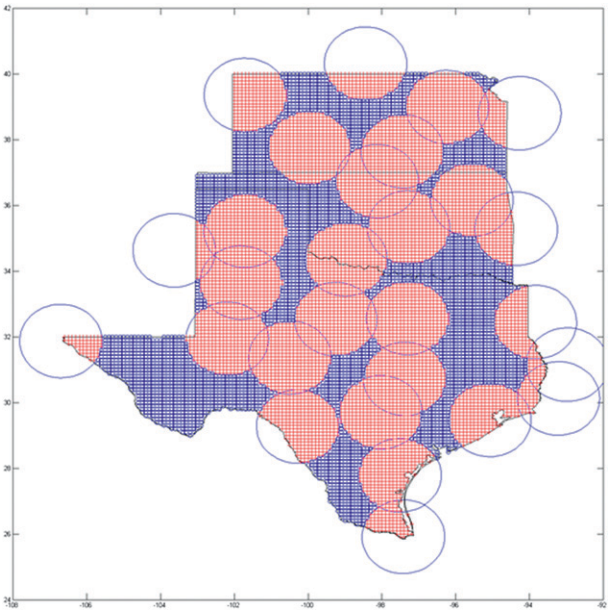

FIG. 1. Graphical representation of real-world boundaries, gridded system, and the method of determining fitness. In a binary example, each of the grid points colored red would be assigned a value of 1 (covered by a radar), and each of the grid points colored blue would be assigned a value of 0. The fitness is determined by adding up these gridpoint values. Also note that each grid point also serves as a potential siting location, limiting the possible sites to a more manageable number for computation.

The fitness function improves for each point that is covered by a radar, resulting in a ''spreading'' effect of the radar locations; this effectively maximizes coverage for the given number of radars. The grid can be enhanced using similarly gridded datasets (or fields), which add value to specific locations. The use of fields will be explored in the first example in section 3.

3. Representative optimization examples

This paper provides three example optimizations, illustrating the flexibility and scope of the algorithm. The first example utilizes both severe weather climatology and population density data to optimize a small, dual-frequency network. The second takes into account X-band attenuation due to average convective rainfall as observed by the Oklahoma Mesonet in the design of a dual-frequency network. The third example demonstrates the ability to incorporate terrain blockage in combined mountainous/flat regions while also optimizing a dual-frequency network. These examples are summarized in Table 1. This section describes the data acquisition, methodology, and results used for each example.

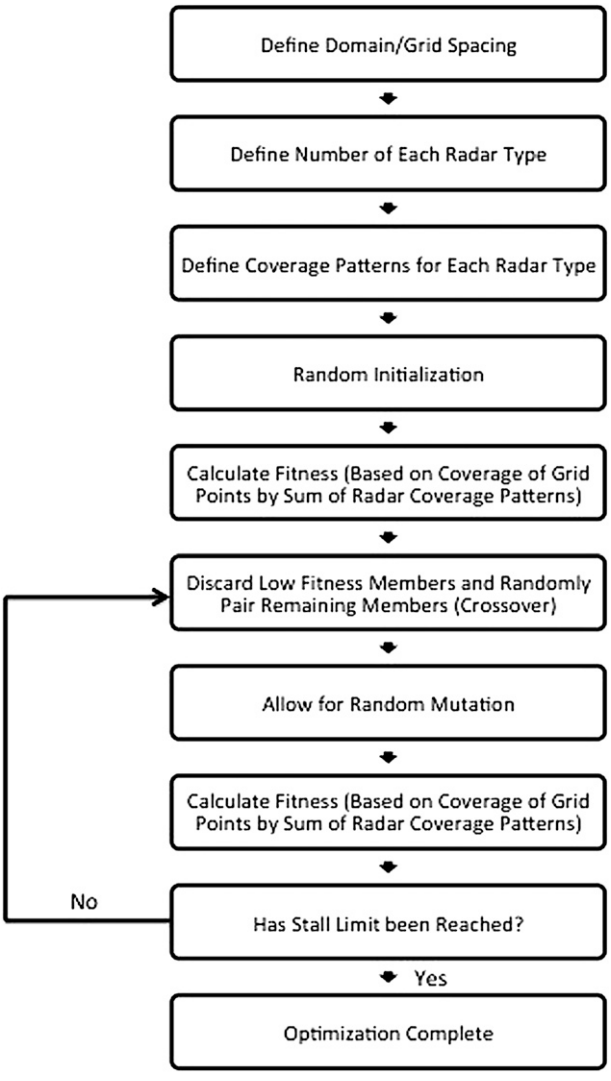

FIG. 2. Flowchart describing the genetic algorithm used for optimization. Fitness is determined by summing the values of the covered grid points, with higher fitness representing a more favorable solution.

a. Population density and tornado climatology: An illustrative example in Indiana

A key feature of the optimization algorithm is the ability to optimize spatially with the aid of a ''field,'' which can be adapted to the grid spacing being used for potential sites. Fields alter the binary system of assessing radar coverage by weighting the fitness score based upon a predetermined variable. A basic example is a multiplicative field of population density and tornado climatology. This results in one optimizable field, which is superimposed over the entire domain to be optimized.

It should be emphasized that the algorithm is flexible enough to accommodate a vast number of possible examples beyond those shown in the following sections. There are a number of optimization criteria that can be chosen for optimization; however, it can be challenging to acquire the necessary data at a high-enough resolution for accurate analysis. Tornado occurrence and population centers are two relevant metrics that can be easily acquired and combined, and allow for an accurate demonstration of nonbinary weighting in a network optimization. It is important to note that any quantifiable data that can be interpolated to the grid system can be used as a field/weighting tool.

1) METHODOLOGY

Population density data are available from many sources and in many formats. The highest resolution data available free of charge were obtained from the Center for International Earth Science Information Network at Columbia University. The Gridded Population of the World project provides population density files spanning the entire earth at a base resolution of 2.5 arc minutes (or approximately 0.0417°) for the year 2000 (Balk and Yetman 2004). A linear combination of Green functions, known as a biharmonic spline interpolation method (Sandwell 1987), is used to degrade the resolution of the data to 0.1° in order to fit the grid spacing used by the optimization algorithm (Fig. 3a).

Additionally, in the midwestern states of the United States, tornado detection at low levels is a serious concern for forecasters. Therefore, it is conceivable that a radar network designer with limited funds would want to weight the placement of radar systems toward those areas more likely to be affected by tornadoes. Tornado climatology data in the form of number of F2 tornado days per year from 1950–2009 (Brooks et al. 2003) are used for this study as input to the grid system (Fig. 3b).

TABLE 1. Three siting optimization examples.

Type	Location	Height AGL	X-band range	Fixed radars?
Combined field	Indiana	1 km	40 km	WSR-88D
Attenuation	Oklahoma	1 km	~25 km	None
Terrain blockage	Colorado	1 km	40 km	None

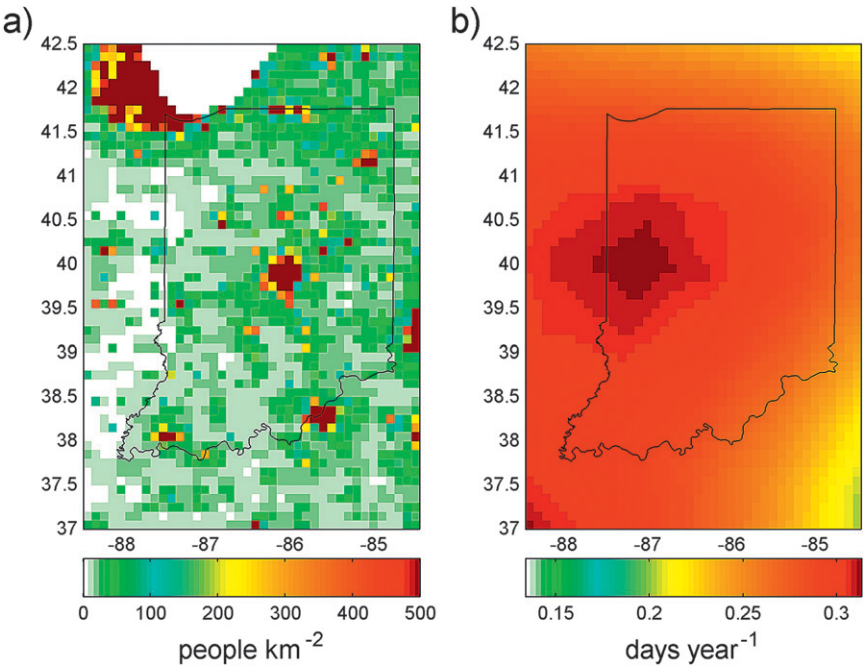

FIG. 3. (a) Population density (people per square kilometer) in the state of Indiana and surrounding areas (from the year 2000). (b) Average number of F2 tornado days per year during 1950–2009 for the same location.

No normalization of the data was used in this case; the raw data points were interpolated to the grid resolution being used by the optimization algorithm (0.1° by 0.1°), and multiplied together, resulting in units of people per square kilometer × days yr^{-1}. The raw data points at the final resolution represent a ''summary'' of each field variable in the given space. As an example in this study, the two fields are multiplied in order to provide one field variable to the algorithm. In other situations, different weighting techniques between available fields may be used to arrive at a final field variable.

2) RESULTS

Figure 4a shows an optimized dual-frequency radar network, with current WSR-88D site locations locked in place (with 1-km vertical coverage, resulting in approximately 60-km range at a 0.5° elevation), and optimizable X-band radars (with 40-km range). The shading in Fig. 4a is the multiplicative field of Figs. 3a,b. Indiana was chosen for this example due to its relatively strong gradient in tornado probability overlapped with moderately high areas of population density, resulting in strongly defined areas warranting coverage. Since low-level coverage is a key influence in any next-generation weather radar network, and WSR-88D locations are already optimized for location, WSR-88D locations are locked in this example, while optimizable X-band radars are used to fill in coverage gaps. In this specific example, it is assumed that the network designer only has 10 X-band radars available to add to the existing network, resulting in the desire to strategically place additional radars in a manner such that the most important areas are covered first.

Figure 4b shows an optimized single-frequency radar network, with 20 optimizable X-band radars. In this example, no current WSR-88D radars were included, allowing for a completely new network design based upon a given field. The field used is identical to that in Fig. 4a, and the available radars are again strategically placed based on the weighting of the field.

It is critical to note that the ''most important'' areas are defined by the field being used, and can be customized by the user. The results in Fig. 4 show that the shaded areas, representing areas of highest population density and tornado probability, are covered first. With limited resources, and therefore the lack of ability to provide full coverage in this example, the available radars provide as much coverage for the population centers as possible.

Additionally, any number of radars may be used for optimization. A network designer can, for example, gather an idea for the number of radars needed to fill the entire state of Indiana, without regard to a field. The field simply serves as a starting point for the placement of the

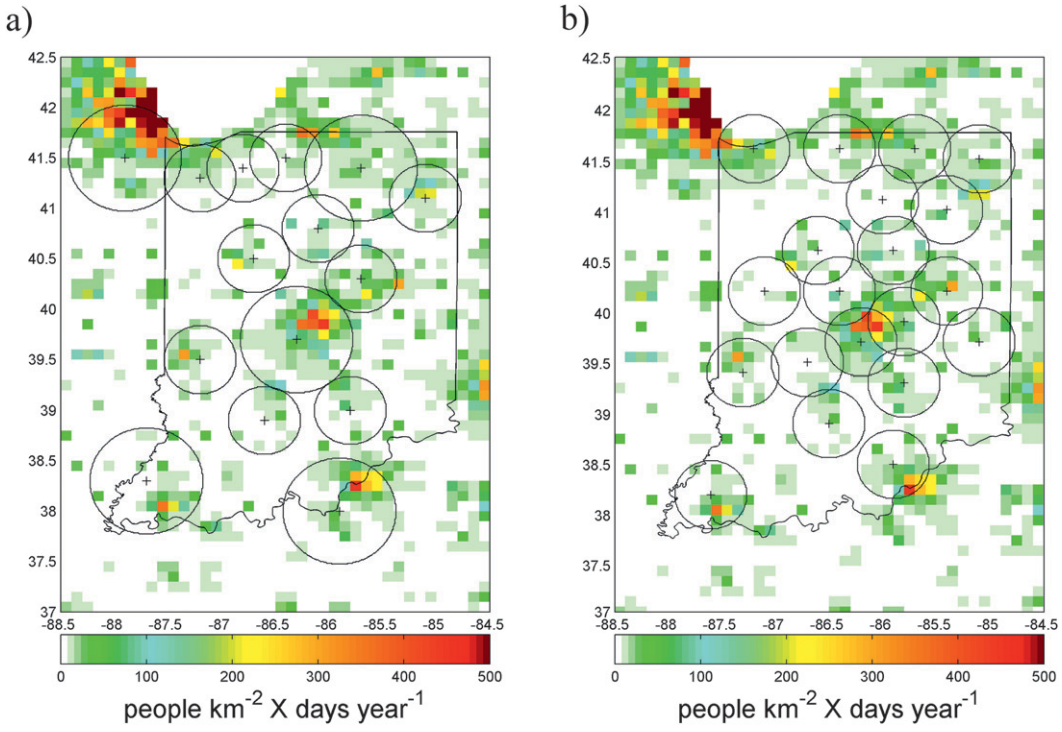

FIG. 4. (a) Optimized dual-frequency radar network for the state of Indiana, using a multiplicative combination of Figs. 3a,b, fixed WSR-88D locations with 1-km vertical coverage maximum, and 10 optimizable X-band radars. (b) Optimized single-frequency radar network for the state of Indiana, using the same field as in (a), but with 20 optimizable X-band radars.

first new radars, in order to cover the areas deemed most important first.

b. *Accounting for attenuation: Use of Mesonet data for an Oklahoma network*

A useful tool for a network optimization is the ability to accurately represent the coverage of a given radar type given a set of atmospheric conditions. In even moderate precipitation cases, X-band coverage range at a reliable sensitivity level can be significantly degraded, resulting in the need for more radars in order to provide data for the same area. Chandrasekar and Lim (2008) proposed dealing with attenuation at high frequencies by incorporating a networked approach, leading to moment estimates (including polarimetric variables) based upon the returned signals to multiple radars. While this technique is applicable to the given scenario, the optimal placement of individual, *nonoverlapping* radars across a wide domain is a key requirement for such a network to operate. The second example is a simple coverage optimization, but utilizes average rainfall data to account for attenuation at X band. This example illustrates the difference in range between clear and precipitating conditions for high-frequency radar systems, and how this difference affects a cost–benefit analysis of a potential multifrequency network.

1) METHODOLOGY

Oklahoma Mesonet data are utilized for this example, and were provided by the Oklahoma Climatological Survey (McPherson et al. 2007). To quantify average ''convective season'' precipitation, 10 years of data from the month of May (May 2001–May 2010) were acquired. These data contain rainfall information at 5-min resolution for well over 100 Mesonet stations across Oklahoma.

Since a change in radar sensitivity with range due to attenuation is only a concern when it is *actually* precipitating, it is not sufficient to simply calculate the amount of rain over the entire period and divide by the total time. Instead, it is prudent to determine the average rainfall rate *only when raining*. To achieve this goal, each 5-min bin is tested for a change of at least 0.01 in. of precipitation. If this condition is met, it is considered to have been raining for the entire length of the 5-min bin. All 10 years of data are processed in this matter, resulting in a total amount of rainfall, as well as a total amount of time in which precipitation was occurring. The quotient of these numbers results in the average rainfall rate during the month of

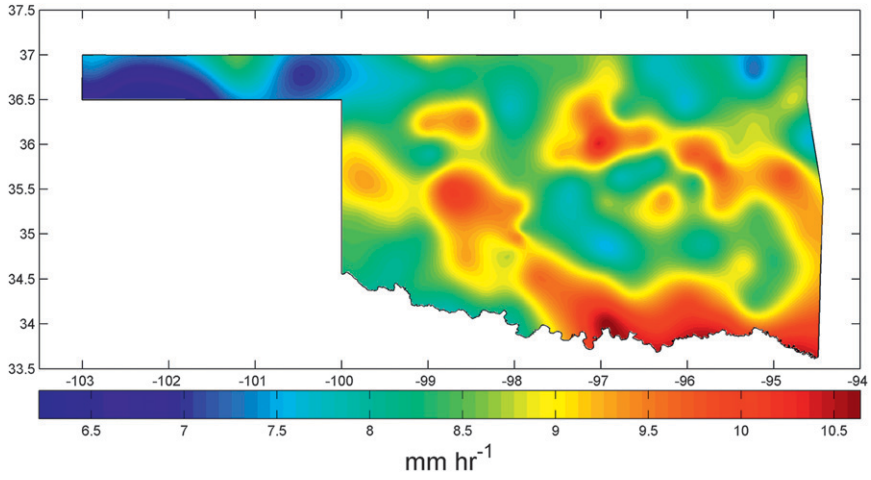

FIG. 5. Average rainfall rate over the state of Oklahoma for the month of May during 2001–10 (mm h^{-1}).

May during 2001–10. This value is calculated for each individual Mesonet station, and a biharmonic spline interpolation (Sandwell 1987) is once again used to interpolate the data to the grid spacing required for analysis (in this case, 0.1° grid spacing is used), as shown in Fig. 5.

Each potential site in the grid is tested for attenuation. The weather radar equation is used to compare the sensitivity of a nonattenuated radar to the sensitivity of a radar that experiences losses due to the rainfall shown in Fig. 5 (Doviak and Zrnić 1993):

$$P_r = \frac{P_t g^2 \eta c \tau \pi \theta^2 \lambda^2}{(4\pi)^3 r^2 l^2 16 \ln 2}, \quad (1)$$

where P_r and P_t are power returned and transmitted, respectively (W); g is gain of the antenna and l represents losses (both in dB); η is reflectivity (m^{-1}); c is the speed of light (m s^{-1}); τ is the pulse width (μs); λ is wavelength and r is range (both in m); and θ is one-way half-power beamwidth. Equation (1) can be solved for η, which can in turn be used to calculate reflectivity factor Z:

$$Z = \frac{r^2 l^2 (4\pi)^3 16 \ln 2 P_r \lambda^2}{P_t g^2 c \tau \pi^6 \theta^2 |k_w|^2}, \quad (2)$$

where k_w is the specific attenuation of water (unitless), and P_r is set to −110 dBm.

Figure 6 shows two profiles that solve for Z with respect to r. The solid line represents a typical X-band radar (e.g., CASA) sensitivity profile with only atmospheric losses taken into account (a nonprecipitating case). At 50 km, for example, the sensitivity of such a radar is approximately 21 dBZ, meaning the *minimum* return that the radar can detect is 21 dBZ. The dashed line represents an example sensitivity profile that takes into account both atmospheric losses and those due to the rainfall rate profile shown. This radar profile reaches the same sensitivity threshold as the atmosphere-only case at 28 km, meaning that the effective range of the radar is cut by 22 km (44%).

This method can be used to compare standard, nonprecipitating radar operating ranges to conditions that incorporate losses due to rainfall, resulting in different effective radar ranges. The technique incrementally checks to see whether the current attenuated range is greater than or less than the current range being tested. If it is less, the increments stop, and the range for the radial being tested is recorded. This is repeated for each radial (at 1.0° increments), resulting in a new coverage pattern for the radar site being tested. This new pattern is based solely on the rainfall rate and associated attenuation, resulting in slightly different coverage patterns throughout the state.

It is important to note that in this example, no fields were used in the optimization; a binary weighting system was used in the fitness function. The difference in this example is that instead of using circles for radar representation based upon height above ground level, the circles plotted and used in the algorithm's computations are representative of X-band losses due to heavy precipitation. For example, a sensitivity range of 50 km was used to determine each radar's effective range after passing through precipitation. These new radar coverage patterns were used as input to the genetic algorithm,

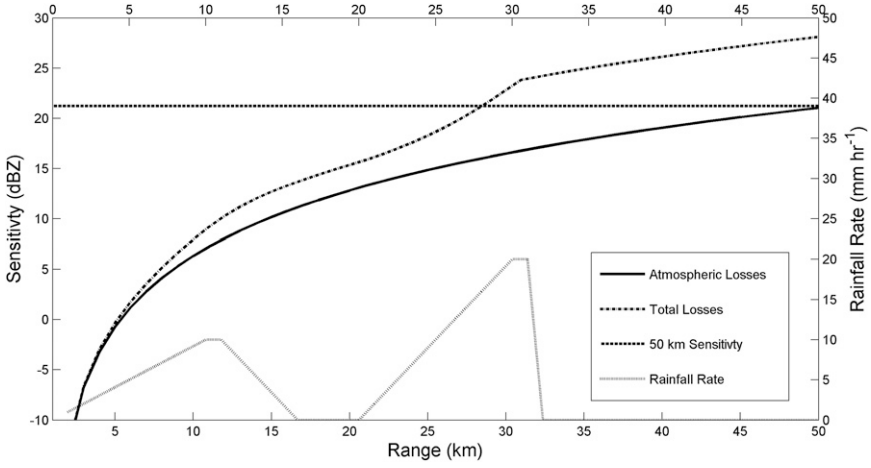

FIG. 6. Sensitivity for a CASA radar based on atmospheric losses compared with sensitivity taking into account both atmospheric losses and losses due to the given rainfall profile with range. The sensitivity at 50 km with only atmospheric losses is displayed, with the profile including rainfall losses reaching the same sensitivity level at approximately 28 km.

which ran as normal on a binary grid, except with smaller effective radar ranges.

2) RESULTS

Figure 7a shows an example optimization in the state of Oklahoma, with 5 optimizable S-band radars at 1-km vertical coverage and 79 optimizable X-band radars. The shading represents the average rainfall rate in mm h^{-1}. Note that the average range of the X-band radars is markedly less than those using the traditional specifications in Fig. 4 (approximately 25 km vs 40 km). Additionally, the S-band radars in this case are *not* locked to current WSR-88D locations.

In a network that aims to cover an entire domain (as opposed to one that uses fields to cover only the most important areas), there are a number of added concerns that are raised for the network designer. In a large domain setting, it is conceivable that an optimal combination of S-band radars and X-band radars (or other frequencies if desired) may be used in order to achieve better coverage, while also limiting cost.

To assess this possibility, the optimization in Oklahoma was repeated for 260 possible combinations of S-band and attenuated X-band radars; the results are shown in Fig. 7b. The blue data points represent incrementally increasing quantities of X-band radars, with a fixed number of zero S-band radars. The green data points represent the same increment of X-band radar quantities; however, the number of S-band radars is fixed at five. The last (most expensive) data point for the 0 S-band curve corresponds to 160 X-band radars, while the last (most expensive) data point for the 5 S-band curve corresponds to 110 X-band radars. The corresponding lines represent a third-order polynomial fit to each set of data.

The abscissa represents 30-yr network cost, with an assumed \$5 million (U.S. dollars) initial cost for the S-band radars, and a \$500,000 initial cost for the X-band radars. Annual maintenance costs are set at \$500,000 and \$50,000 for the S band and X band, respectively. The S-band costs were determined using a combination of recent S-band radar sales figures, as well as estimations provided by the Radar Operations Center, the Office of the Federal Coordinator for Meteorology, and McLaughlin et al. (2009). The X-band costs were estimated using approximate values from McLaughlin et al. (2009); however, the values provided were adjusted to approximately account for profit margins and estimated manpower. It is critical to note that these numbers are simply rough estimates for system costs and maintenance. The dollar costs can easily be changed for cost-benefit analysis purposes.

The ordinate represents the number of grid points covered in each optimization. Each point represents approximately 107 km^2 at 30°N latitude (111.0 km per degree of latitude, and 96.5 km per degree of longitude), resulting in maximum coverage corresponding to approximately 1750 grid points, or about 187 250 km^2. Because of the circular shape of each radar's coverage area, as well as leakage of each grid point around the boundaries of the state, the resultant estimated coverage is slightly higher than the total area of the state (181 195 km^2).

The analysis shows that while using the estimated dollar costs for each radar type, an increase in possible coverage exists for every dollar amount by using only

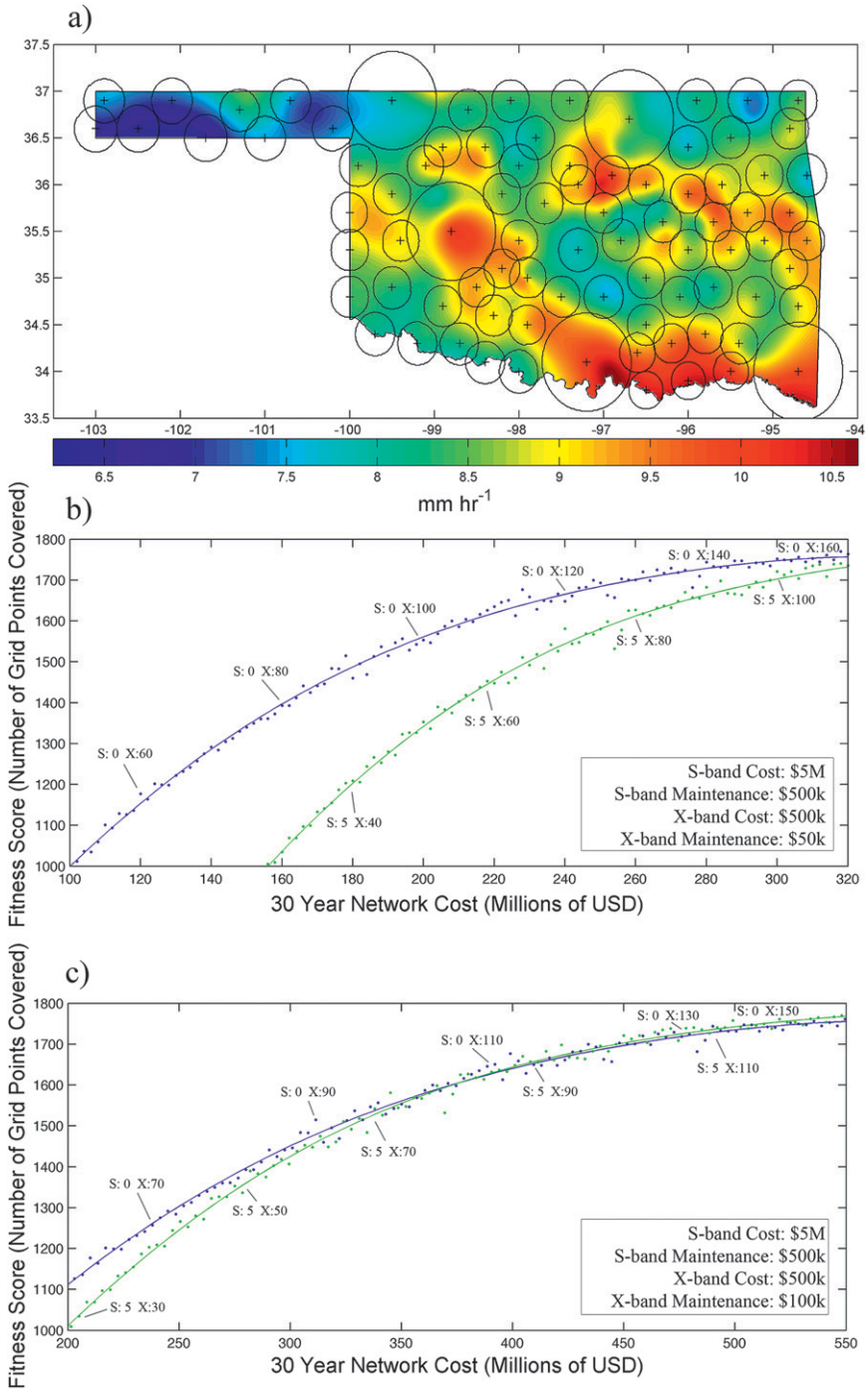

FIG. 7. (a) Optimized dual-frequency radar network for the state of Oklahoma, using 5 S-band radars at 1-km vertical coverage, and 79 X-band radars with coverage patterns based on average rainfall rate for the month of May during 2001–10 (shaded, mm h^{-1}). (b) 30-yr network total cost–benefit analysis of 260 combinations of S- and X-band radar configurations in the state of Oklahoma, with aforementioned attenuation taken into account. The blue points and curve represent incrementally increasing number of X-band radars, with zero S-band radars; the green points and curve represent the same, but with five S-band radars. S-band initial cost and maintenance are assumed to be $5 million and $500,000, respectively, while X-band initial cost and maintenance are assumed to be $500,000 and $50,000, respectively. (c) As in (b), but with X-band maintenance cost of $100,000.

X-band radars, rather than using five S-band radars, mixed with the corresponding number of X-band radars. The peak differential between the curves occurs at an approximately \$160 million network cost, with a gap of approximately 300 grid points, equivalent to 32 100 km^2. Additionally, the zero S-band curve reaches the approximate coverage maximum at about \$280 million, while the five S-band curve does not reach the same corresponding level until approximately \$320 million. This results in a 30-yr network cost savings of approximately \$40 million needed to cover the entire state, with the dollar costs being used.

It is of critical importance to note that this cost model is elementary in nature, and in no way represents a definitive cost model for future radar networks. This example is meant to demonstrate the *capability* to apply algorithm output to a cost model. This is an important feature of the algorithm, since no additional computations are needed within the optimization to apply varying levels of cost models. A second example, shown in Fig. 7c, represents the exact same algorithm simulations, but with an X-band annual maintenance cost of \$100 thousand (twice that of the first example). While such a cost for annual maintenance is likely too high, the marked difference between curves is immediately apparent. Instead of a distinct advantage for X-band-only networks, the two curves converge as they approach optimal coverage, leading to a very different result than what is shown in Fig. 7b. Additionally, this result has been computed using a relatively low-level coverage height for S-band radars. An extension in coverage range would change these results considerably.

These examples demonstrate the ability to change network design figures on the fly based on a change in expected budget, as well as the drastic changes that can occur when choosing a different cost model. A significantly more complicated model can easily be applied to previous algorithm output. The desire to pursue such modeling is expressed in section 4.

c. *Terrain blockage: A network in Colorado*

Obtaining radar coverage in mountainous regions can be a difficult challenge for network designers. Despite the current lack of low-level weather radar coverage in the Rocky and Appalachian Mountains, it is plausible to expect a next-generation radar network will attempt to offer significantly higher coverage areas across these regions. Of principle interest in a network utilizing high-frequency, low-power radar systems is the ability to cover these areas of complex terrain. This problem has been documented by Brotzge et al. (2009), pointing to the need for a computationally simple method to account for terrain blockage in radar network design and optimization. This example explores the use of a terrain analysis tool in optimizing for comprehensive coverage in Colorado.

1) METHODOLOGY

Terrain data must be selected, and as with population density data, a number of sources are available. This paper utilizes Global 30 Arc-Second Elevation Data Set (GTOPO30) data provided by the U.S. Geological Survey, at a resolution of 30 arc seconds (or approximately 0.0083°). Unlike the population density data, the terrain data are not degraded in resolution and used in the optimization grid. Instead, the data are processed through a separate terrain analysis algorithm, which assesses the resultant blockage at each potential radar site defined by the gridded system (while using the full-resolution terrain data for analysis). At each grid point, a 4/3 law is used for propagation (Doviak and Zrnić 1993):

$$h = (r^2 + a_e^2 + 2ra_e \sin\theta_e)^{1/2} - a_e, \tag{3}$$

where h is height, r is range, and a_e is the effective earth's radius (4/3 the earth's radius), all in km, and θ_e is the elevation angle.

The theoretical beam is propagated in 1.0-km range gates, until one of three stopping criteria are met:

1) The height of the beam is lower than the current elevation.
2) The height of the beam is higher than a predetermined cutoff height.
3) The distance from the radar site exceeds the theoretical range limits set by the antenna frequency and power.

When the height of the beam is lower than the current elevation, a ground obstruction has been encountered, and the beam can no longer propagate further. The predetermined cutoff height allows the user to define the maximum allowable height that the beam may be above ground level, resulting in the ability to specify parameters to achieve the low-level coverage desired. The theoretical range limits are calculated using a combination of current operational radar range limits and comparisons via Eq. (1).

For all of the analyses, a 0.5° elevation angle and a tower height of 30 m were used. The method is repeated for each radial (at 1.0° intervals), and the results are stored for later use by the optimization algorithm. The results can be plotted for each radar site, offering the user the expected coverage limits for a given radar at a given potential site. An example is shown in Fig. 8;

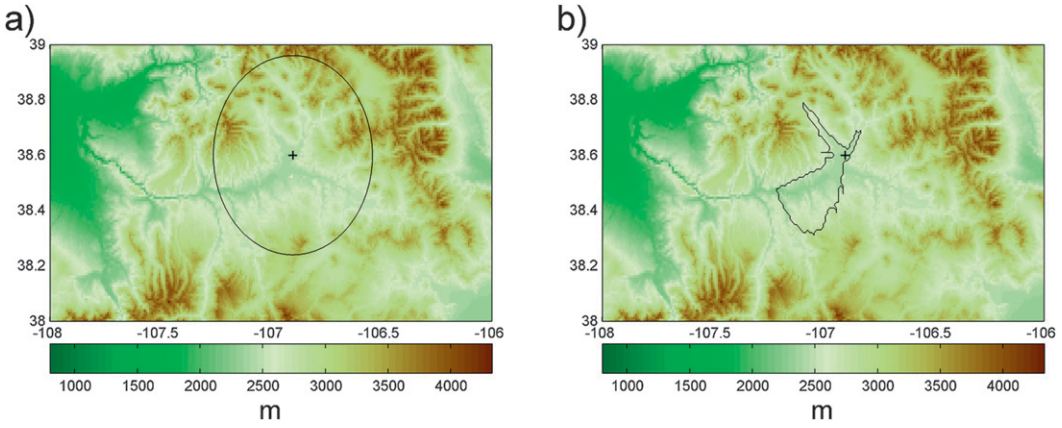

FIG. 8. (a) General coverage model of an X-band radar in Colorado. (b) Coverage model that takes into account terrain blockage.

note that the boundaries of the radar coverage are no longer necessarily circular, but conform to the limitations that arise from the terrain map.

Once inserted into the final optimization algorithm, the new boundaries are used for a given radar site instead of the more simplistic circular boundary. Only grid points which fall within the new boundaries are counted as being covered by the radar in question, resulting in a more accurate representation of radar coverage in mountainous regions.

2) RESULTS

A series of potential single- and dual-frequency radar networks are optimized for the state of Colorado, while taking into account changes in coverage patterns due to terrain blockage at each individual radar site. Figure 9a shows an example optimization, with 15 S-band radars at 1-km vertical coverage, and 76 X-band radars. The S-band radars are characterized by translucent white coverage areas, while X-band radars are represented by translucent yellow coverage areas. The shading is representative of the terrain height above mean sea level, in meters. The algorithm optimizes this case in the same manner as the Oklahoma attenuation example (a binary grid system), but with coverage patterns based upon the terrain map.

Radars are strategically placed to avoid mountain ridges with this strategy due to the implementation of the radar height equation at each possible radar site. Item 2) in the list of stopping criteria in the previous section allows the user to ensure that the height of the beam is not above a given threshold. Since a 0.5° elevation angle is used in this example, it would be impractical to place a radar on a mountain ridge, since the height of the beam would be well over the 1-km vertical coverage threshold rather quickly. In future studies, specifically in a national radar network, it will become critical to account for additional base elevation levels, similar to the negative-angle techniques proposed by Brown et al. (2002).

Similar optimizations are repeated for 315 combinations of S-band and X-band radars, with the results shown in Fig. 9b. The blue data points represent incrementally increasing quantities of X-band radars, with a fixed number of zero S-band radars. The green data points represent the same increment of X-band radar quantities; however, the number of S-band radars is fixed at 15. The last data point for the zero S-band curve corresponds to 170 X-band radars, while the last data point for the 15 S-band curve corresponds to 135 X-band radars. The corresponding lines represent a third-order polynomial fit to each set of data, and radar costs, both initial and maintenance, are set at the same levels used in the first Oklahoma attenuation example (Fig. 7b, $5 million initial cost and $500,000 annual maintenance for S-band radars; $500,000 initial cost and $50,000 annual maintenance for X-band radars).

The zero S-band data appear above the 15 S-band data, resulting in more cost-efficient network designs without the use of S-band radars. The reasons for this difference are varied; however, the principle causes are the lack of rainfall attenuation consideration, as well as the varied terrain of the region. Without taking into account attenuation for X-band radars, the range is considerably higher (40 km vs approximately 25 km), before considering terrain blockage. S-band vertical height coverage of 1 km also significantly hurts the S-band cause in this case; a higher limit would move the curves closer together. Additionally, X-band radars are commonly used in the optimization algorithm to provide relatively small areas of coverage for a lower cost. S-band radars do not appear in many of these locations because of

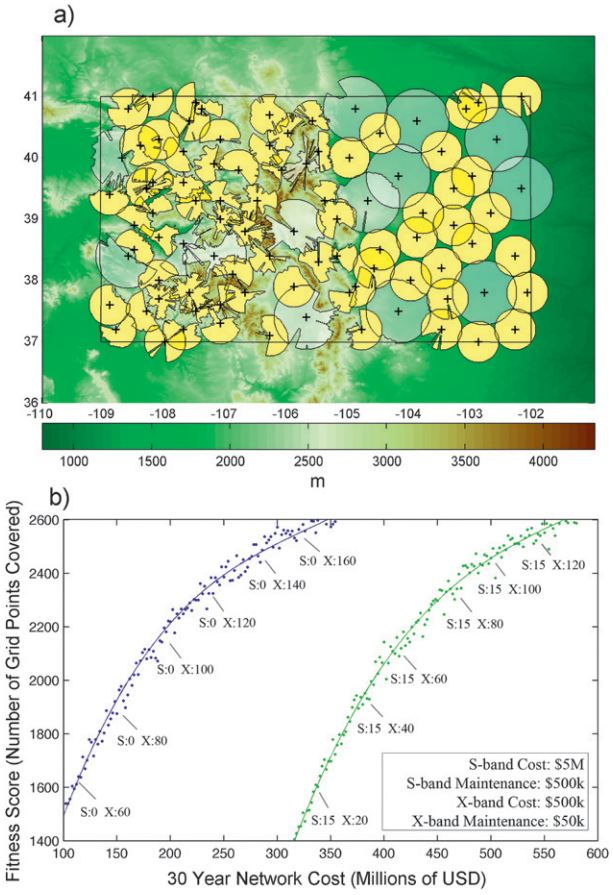

FIG. 9. (a) Optimized dual-frequency radar network for the state of Colorado, using 15 S-band radars at 1-km vertical coverage, and 76 X-band radars with coverage patterns based on terrain blockage (terrain is shaded, in m above sea level). (b) A 30-yr network total cost–benefit analysis of 315 combinations of S- and X-band radar configurations in the state of Colorado, with aforementioned attenuation taken into account. The blue points and curve represent incrementally increasing number of X-band radars, with zero S-band radars; the green points and curve represent the same, but with 15 S-band radars. S-band initial cost and maintenance are assumed to be $5 million and $500,000, respectively, while X-band initial cost and maintenance are assumed to be $500,000 and $50,000, respectively.

significant terrain blockage, and the resultant lack of a poor cost–benefit ratio.

At 40°N latitude, 1° of longitude is approximately equal to 85.4 km, resulting in an approximate grid equivalent of 94 km^2. With a total area of 269 837 km^2, an expected maximum coverage value, in terms of grid points covered, is equal to about 2870. In this case, reaching the maximum coverage for the domain is considerably slower and more expensive, because of the nature of terrain features. Once the primary, less complex areas are covered, the addition of a single X-band radar results in much less coverage per dollar spent because of terrain blockage.

As with previous examples, it is critical to view these results in terms of the cost model and physical parameters being used. A higher vertical cutoff height for the S-band radars, lower S-band costs, or higher X-band costs would significantly alter the results. The fact that the cost parameters can be easily changed, without rerunning the optimization algorithm, demonstrates the flexibility of the algorithm for a network designer with a fluctuating budget.

4. Conclusions and future work

Radar network design can be represented as a coverage optimization problem, and solved in a vast number of different ways using a wide array of tools. In utilizing a genetic algorithm, network designers in a variety of different situations can be offered an objective approach in terms of potential cost–benefit fields and analyses. Radar networks can be optimized based on fields of interest in order to place radars in locations with the highest cost–benefit ratio first (covering areas with high importance results in high ''benefit''). Radar coverage patterns for individual potential sites can be altered to reflect atmospheric conditions, terrain blockage, or other site-specific or full-domain parameters. Networks can also be optimized across multiple designs (e.g., frequency, sensitivity, etc.) in an attempt to offer an estimate of the most cost-efficient combination of radar types.

In addition to the examples shown, a vast number of possibilities exist for experimentation and analysis. *Any* quantifiable field that can be adapted to the grid spacing being used for siting locations can be used to optimize a radar network, and any combination of frequencies can be used for full-domain cost–benefit analysis. System costs, both initial and maintenance, are alterable after network optimizations have been completed, resulting in minimal computational requirements needed for changes to a budget.

With the structure of the algorithm completed, a number of possible scenarios are under consideration for analysis. Work is currently under way attempting to synthesize MPAR and ''Terminal'' MPAR requirements, in order to accurately determine the number of S-band MPAR radars that would be needed in a next-generation weather and aircraft sensing network (Weber et al. 2007). Different cost models, as well as the use of negative elevations angles, are also under consideration for application to these results. Also, we are looking into how different vertical height coverage values would change our results. A method for comparing 1-, 2-, and 3-km vertical height coverages on a regional or national scale is planned. We hope to

present national-scale radar network cost and design results in the near future using our algorithm.

Additionally, applications of hydrological fields, combined with terrain blockage at a high resolution, is a desired step for the future. Urban flooding events in mountainous regions and watersheds present a significant problem for forecasters, and accurate quantitative precipitation estimation provided by small, inexpensive, high-frequency optimized weather radar networks is a possible method to assist in the efforts to warn the public in a timely matter. These efforts, along with others, may be achievable using radar networks to enhance numerical weather prediction methods, as well as to provide real-time observational data. Finally, the desire to have overlapping coverage in certain areas is a necessary development step for the algorithm, with strong emphasis on the need for dual-Doppler coverage in some areas of the country. This goal will be critical in working toward the future goal of providing warn-on-forecast tornado and severe thunderstorm warnings.

Acknowledgments. This work was partially supported by the National Severe Storms Laboratory (NOAA/NSSL) under Cooperative Agreement NA17RJ1227. We thank Harold Brooks for supplying us with the tornado climatology data used in this study, as well as the staff at the Oklahoma Climatological Survey for providing Mesonet data for our attenuation studies. We are also grateful for the continued assistance from Brett Zimmerman and the rest of the staff at the University of Oklahoma Supercomputing Center for Education and Research (OSCER), in addition to the help from Boon Leng Cheong with the application of radar sensitivity to attenuation. Finally, the authors thank the anonymous reviewers of this paper for helping to improve the manuscript before publication.

REFERENCES

Amaldi, E., A. Capone, and F. Malucelli, 2008: Radio planning and coverage optimization of 3G cellular networks. *Wireless Network,* **14,** 435–447.

Balk, D. T., and G. Yetman, 2004: The global distribution of population: Evaluating the gains in resolution refinement. Tech. Rep., Center for International Earth Science Information Network, Columbia University, Palisades, NY, 15 pp.

Boender, C. G. E., A. H. G. Rinnooy Kan, L. Strougie, and G. T. Timmer, 1982: A stochastic method for global optimization. *Math. Program.,* **22,** 125–140.

Brooks, H. E., C. A. Doswell III, and M. P. Kay, 2003: Climatological estimates of local tornado probability for the United States. *Wea. Forecasting,* **18,** 626–640.

Brotzge, J., R. Contreras, B. Philips, and K. Brewster, 2009: Radar feasibility study. NOAA Tech. Rep., 130 pp. [Available from J. Brotzge, 120 David L. Boren Blvd., Ste. 2500, University of Oklahoma, Norman, OK 73072-7309.]

Brown, R. A., V. T. Wood, and T. W. Barker, 2002: Improved detection using negative elevation angles for mountaintop WSR-88Ds: Simulation of KMSX near Missoula, Montana. *Wea. Forecasting,* **17,** 223–237.

Celis, M., J. E. Dennis, and R. A. Tapia, 1984: A trust region strategy for equality constrained optimization. *Proc. Conf. on Numerical Optimization,* Tech. Rep. 84-1, Boulder, CO, SIAM, 15 pp. [Available online at http://www.caam.rice.edu/caam/trs/84/TR84-01.pdf.]

Chandrasekar, V., and S. Lim, 2008: Retrieval of reflectivity in a networked radar environment. *J. Atmos. Oceanic Technol.,* **25,** 1755–1767.

Dantzig, G. B., and M. N. Thapa, 1997: *Linear Programming: 1: Introduction.* Springer Series in Operations Research and Financial Engineering, Vol. 1, Springer, 473 pp.

Doviak, R., and D. Zrnić, 1993: *Doppler Radar and Weather Observations.* 2nd ed. Academic Press, 562 pp.

Du, L., and J. Bigham, 2003: Constrained coverage optimisation for mobile cellular networks. *Proc. Int. Conf. on Applications of Evolutionary Computing,* Essex, United Kingdom, EvoWorkshops 03, 199–210.

Eiben, A. E., and J. E. Smith, 2007: *Introduction to Evolutionary Computing.* 2nd ed. Springer, 316 pp.

Holland, J., 1975: *Adaption in Natural and Artificial Systems: An Introductory Analysis with Applications to Biology, Control, and Artificial Intelligence.* The University of Michigan Press, 211 pp.

Jourdan, D. B., and O. L. de Weck, 2004: Layout optimization for a wireless sensor network using a multi-objective genetic algorithm. *Proc. IEEE 59th Vehicular Technology Conf.,* Vol. 5, Milan, Italy, IEEE, 2466–2470.

Karmarkar, N., 1984: A new polynomial time algorithm for linear programming. *Combinatorica,* **4,** 373–395.

Leone, D. A., R. M. Endlich, J. Petričeks, R. T. H. Collis, and J. R. Porter, 1989: Meteorological considerations used in planning the NEXRAD network. *Bull. Amer. Meteor. Soc.,* **70,** 4–13.

Lieska, K., E. Laitinen, and J. Lähteenmäki, 1998: Radio coverage optimization with genetic algorithms. *Proc. IEEE Int. Symp. Personal, Indoor, and Mobile Radio Comm.,* Vol. 1, Boston, MA, IEEE, 318–322.

McLaughlin, D., and Coauthors, 2009: Short-wavelength technology and the potential for distributed networks of small radar systems. *Bull. Amer. Meteor. Soc.,* **90,** 1797–1817.

McPherson, R. A., and Coauthors, 2007: Statewide monitoring of the mesoscale environment: A technical update on the Oklahoma Mesonet. *J. Atmos. Oceanic Technol.,* **24,** 301–321.

Minciardi, R., R. Sacile, and F. Siccardi, 2003: Optimal planning of a weather radar network. *J. Atmos. Oceanic Technol.,* **20,** 1251–1263.

Nelder, J. A., and R. Mead, 1965: A simplex method for function minimization. *Comput. J.,* **7,** 308–313.

Raisanen, L., and R. M. Whitaker, 2003: Multi-objective optimization in area coverage problems for cellular communication networks: Evaluation of an elitist evolutionary strategy. *Proc. ACM Symp. on Applied Computing,* Melbourne, FL, SIGAPP, 714–720.

Ray, P. S., and K. L. Sangren, 1983: Multiple-Doppler radar network design. *J. Appl. Meteor. Climatol.,* **22,** 1444–1454.

Sandwell, D. T., 1987: Biharmonic spline interpolation of GEOS-3 and SEASAT altimeter data. *Geophys. Res. Lett.,* **14,** 139–142.

Shanno, D. F., 1970: Conditioning of Quasi-Newton methods for function minimization. *Math. Comput.,* **24,** 647–656.

Stensrud, D. J., and Coauthors, 2009: Convective-scale warn-on-forecast system: A vision for 2020. *Bull. Amer. Meteor. Soc.,* **90,** 1487–1499.

Thornton, J., D. Grace, M. H. Capstick, and T. C. Tozer, 2003: Optimizing an array of antennas for cellular coverage from a high altitude platform. *IEEE Trans. Wireless Commun.,* **2,** 484–492.

Weber, M. E., J. Y. N. Cho, J. S. Herd, J. M. Flavin, W. E. Benner, and G. S. Torok, 2007: The next-generation multimission U.S. surveillance radar network. *Bull. Amer. Meteor. Soc.,* **88,** 1739–1751.

Yussouf, N., and D. J. Stensrud, 2008: Impact of high temporal frequency radar data assimilation on storm-scale NWP model simulations. Preprints, *24th Conf. on Severe Local Storms,* Savannah, GA, Amer. Meteor. Soc., 9B.1. [Available online at http://ams.confex.com/ams/24SLS/techprogram/paper_141555.htm.]

Zrnić, D. S., and Coauthors, 2007: Agile-beam phased array radar for weather observations. *Bull. Amer. Meteor. Soc.,* **88,** 1753–1766.